The p90 ribosomal S6 kinase–UBR5 pathway controls Toll-like receptor signaling via miRNA-induced translational inhibition of tumor necrosis factor receptor–associated factor 3

Received for publication, March 8, 2017, and in revised form, May 18, 2017 Published, Papers in Press, May 30, 2017, DOI 10.1074/jbc.M117.785170

Jin Hwa Cho[‡§], **Sung Ah Kim**[§¶], **Yeon-Soo Seo**[‡], **Sung Goo Park**[§¶], **Byoung Chul Park**[§‖1], **Jeong-Hoon Kim**[¶**2], **and Sunhong Kim**[§‡‡3]

From the [‡]*Department of Biological Sciences, Korea Advanced Institute of Science and Technology, Daejeon 34141, Republic of Korea, the* [§]*Disease Target Structure Research Center, Korea Research Institute of Bioscience and Biotechnology, Daejeon 34141, Republic of Korea,* [¶]*Department of Functional Genomics, School of Bioscience, Korea Research Institute of Bioscience and Biotechnology,University of Science and Technology, Daejeon 34113, Republic of Korea, the* [‖]*Department of Bioanalytical Science, School of Bioscience, Korea Research Institute of Bioscience and Biotechnology, University of Science and Technology, Daejeon 34113, Republic of Korea, the* [**]*Personalized Genomic Medicine Research Center, Korea Research Institute of Bioscience and Biotechnology, Daejeon 34141, Republic of Korea, and the* [‡‡]*Department of Biomolecular Science, School of Bioscience, Korea Research Institute of Bioscience and Biotechnology, University of Science and Technology, Daejeon 34113, Republic of Korea*

Edited by Ronald C. Wek

MicroRNAs (miRNAs) are small, noncoding RNAs that post-transcriptionally regulate gene expression. For example, miRNAs repress gene expression by recruiting the miRNA-induced silencing complex (miRISC), a ribonucleoprotein complex that contains miRNA-engaged Argonaute (Ago) and the scaffold protein GW182. Recently, ubiquitin–protein ligase E3 component N-recognin 5 (UBR5) has been identified as a component of miRISC. UBR5 directly interacts with GW182 proteins and participates in miRNA silencing by recruiting downstream effectors, such as the translation regulator DEAD-box helicase 6 (DDX6) and transducer of ERBB2,1/2,2 (Tob1/2), to the Ago–GW182 complex. However, the regulation of miRISC-associated UBR5 remains largely elusive. In the present study, we showed that UBR5 down-regulates the levels of TNF receptor-associated factor 3 (TRAF3), a key component of Toll-like receptor signaling, via the miRNA pathway. We further demonstrated that p90 ribosomal S6 kinase (p90RSK) is an upstream regulator of UBR5. p90RSK phosphorylates UBR5 at Thr^{637}, Ser^{1227}, and Ser^{2483}, and this phosphorylation is required for the translational repression of TRAF3 mRNA. Phosphorylated UBR5 co-localized with GW182 and Ago2 in cytoplasmic speckles, which implies that miRISC is affected by phospho-UBR5. Collectively, these results indicated that the p90RSK–UBR5 pathway stimulates miRNA-mediated translational repression of TRAF3. Our work has added another layer to the regulation of miRISC.

MicroRNAs (miRNAs)[4] consist of ~21–25–nucleotide, small, noncoding RNAs that post-transcriptionally regulate gene expression. miRNAs are initially transcribed as long primary transcripts that are processed sequentially by Drosha and Dicer enzymes to produce mature miRNA duplex. One strand of the mature miRNA is incorporated into an Argonaute (Ago) family protein in the miRNA-induced silencing complex (miRISC). After loading, miRNA guides the miRISC to its target mRNA through partial base pairing with complementary sites located mostly in the 3′-untranslated region (UTR) of the target mRNA and leads to mRNA degradation and/or translational repression (1). The miRISC consists of miRNA, Ago, GW182, and accessory proteins. Association of Ago–GW182 with downstream effector protein determines how to control miRNA-mediated gene suppression. The GW182 proteins play a central role in target mRNA degradation process by interacting with Ago in miRISC (2). GW182 proteins recruit the PAN2–PAN3 and CAF1–CCR4–NOT deadenylase complexes to miRNA targets through direct interaction with PAN3 and NOT, thereby promoting target mRNA deadenylation and decapping (3). In addition to accelerating mRNA degradation, GW182 is also involved in translational repression through

This work was supported by Grant CAP-15-11-KRICT from the National Research Council of Science and Technology, Ministry of Science, ICT, and Future Planning, Korea and by a grant from the KRIBB (Korea Research Institute of Bioscience and Biotechnology) Research Initiative Program. The authors declare that they have no conflicts of interest with the contents of this article.

This article contains supplemental Figs. 1–5 and Tables 1 and 2.

[1] To whom correspondence may be addressed: Disease Target Structure Research Center, Korea Research Institute of Bioscience and Biotechnology, Daejeon 34141, Republic of Korea. Tel.: 82-42-860-4260; E-mail: parkbc@kribb.re.kr.

[2] To whom correspondence may be addressed: Personalized Genomic Medicine Research Center, Korea Research Institute of Bioscience and Biotechnology, Daejeon 34141, Republic of Korea. Tel.: 82-42-860-4264; E-mail: jhoonkim@kribb.re.kr.

[3] To whom correspondence may be addressed: Disease Target Structure Research Center, Korea Research Institute of Bioscience and Biotechnology, Daejeon 34141, Republic of Korea. Tel.: 82-42-860-4278; E-mail: sunhong@kribb.re.kr.

[4] The abbreviations used are: miRNA, microRNA; miRISC, miRNA-induced silencing complex; Ago, Argonaute; p90RSK, p90 ribosomal S6 kinase; RSK CA, constitutively active p90RSK; PABP, poly(A)-binding protein; TLR, Toll-like receptor; TBK1, TANK-binding kinase 1; PTM, post-translational modification; S6K, p70 ribosomal S6 kinase; SGK, serum and glucocorticoid-regulated kinase; CBS, Coomassie Blue staining; Luc, luciferase; qPCR, real-time PCR; PMA, phorbol 12-myristate 13-acetate.

This is an open access article under the CC BY license.

© 2017 by The American Society for Biochemistry and Molecular Biology, Inc. Published in the U.S.A.

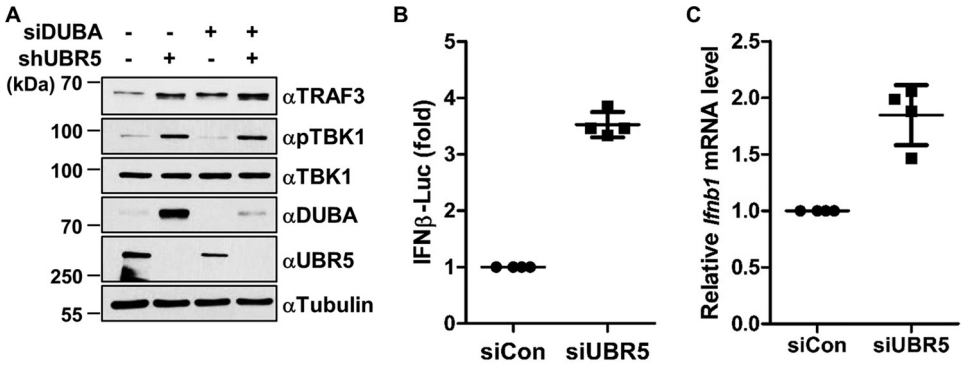

Figure 1. UBR5 negatively regulates TRAF3–TBK1 signaling by a DUBA-independent mechanism. *A*, immunoblot analysis using whole-cell lysate of control or UBR5 shRNA stable HeLa cell lines transfected with control or DUBA siRNA for 48 h. pTBK1 indicates the phospho-Ser[172] TBK1 antibody. All of the immunoblots were completed using the same cell lysates. Data are representatives of three independent experiments. *B*, the Dual-Luciferase assay for the IFNβ gene promoter were completed from the HeLa cell lysates 72 h after transfection with control (*siCon*) or UBR5 siRNA (*siUBR5*) as described under "Experimental procedures." Data are shown as the mean ± S.D. of four samples from a representative experiment performed three times. *C*, qPCR analysis of the *Ifnb1* mRNA level in control or UBR5 siRNA–transfected HeLa cells. Data are shown as the mean ± S.D. of four samples from a representative experiment performed three times.

recruiting the CCR4–NOT complex and DEAD-box ATPase DDX6 (4, 5). GW182 also interact with poly(A)-binding protein (PABP) (6). PABP circularizes mRNA by interacting with both eIF4G (scaffold protein of eIF4F complex) and poly(A) tail to promote translation initiation (6, 7). The GW182–PABP interaction represses translation by interfering with mRNA circularization (6).

UBR5 (also known as EDD), one of the E6–AP carboxyl-terminal (HECT)-type E3 ubiquitin ligase, is originally isolated as a progestin-induced gene in breast cancer cell (8). To date, many proteins have been identified as ubiquitinated substrates and interacting partners for UBR5, through which UBR5 has been shown to be involved in the various cellular processes such as DNA damage responses (9–12), cell cycle progression (13–16), regulation of transcription (17), translation (18), and IL-17 production (19). In Th17 cells, the DUBA–UBR5 axis regulates the stability of transcription factor RORγt and IL-17 production (19). DUBA, an ovarian tumor domain containing deubiquitinase, has been identified as a negative regulator of type I interferon (IFN) production (20). DUBA selectively binds and cleaves Lys[63]-linked polyubiquitin chains on TRAF3 to suppress Toll-like receptor (TLR)-induced type I IFN production but does not affect NF-κB activation (20, 21).

In the present study, we showed that the p90 ribosomal S6 kinase (p90RSK)–UBR5 pathway negatively regulates the translation of TRAF3 through miRNA-mediated translational repression. Depletion of UBR5 increased the level of TRAF3 proteins and the activity of the TRAF3 3′-UTR reporter construct leading to the activation of TRAF3 signaling. Upon stimulation, activated p90RSK directly phosphorylates UBR5 at Thr[637], Ser[1227], and Ser[2483]. In addition, the expression of TRAF3 and KRAS 3′-UTR–containing luciferase reporters was also increased by the inhibition of p90RSK, suggesting that the p90RSK–UBR5 pathway regulates the action of miRNA in general. Finally, the phosphorylated UBR5 by p90RSK was localized at distinct cytoplasmic speckles with Ago2 and GW182. These results indicate that the p90RSK–UBR5 signaling pathway is required for the translational repression by miRNA.

Results

UBR5 negatively regulates TRAF3–TBK1 signaling in a DUBA-independent manner

TRAF3 is one of the substrates for DUBA in TLR-mediated type I IFN production (20). To elucidate the roles of UBR5 in the regulation of TRAF3-mediated TLR signaling, we generated HeLa cell lines stably expressing shRNA targeting control or UBR5. Then, the cells were transiently transfected with siRNA targeting control or DUBA to investigate TRAF3 signaling pathway. The depletion of either UBR5 or DUBA in HeLa cells resulted in an increase in TRAF3 protein level (Fig. 1*A*, *topmost panel*). It has been demonstrated that the Lys[63]-linked polyubiquitin chains of TRAF3 recruit and activate TANK-binding kinase 1 (TBK1) upon viral infection (20, 22, 23). Although overexpression of TRAF3 in epithelial cells can promote the phosphorylation of TBK1 (supplemental Fig. 1) and the production of IFN-β (24), the increased TRAF3 in DUBA knockdown cells did not induce the phosphorylation of TBK1 (Fig. 1*A*), consistent with a previous study (20). On the contrary, UBR5 knockdown significantly induced the up-regulation of the TRAF3 protein level and TBK1 activation loop phosphorylation (Fig. 1*A*). Furthermore, UBR5 depletion increased the activity of the IFNβ reporter (Fig. 1*B*) and the expression of *Ifnb1* mRNA in HeLa cells (Fig. 1*C*). These data suggest that UBR5 negatively regulates TRAF3 in a DUBA-independent manner.

UBR5 regulates TRAF3 expression through miRNA-mediated translational repression

To investigate the mechanism by which UBR5 regulates TRAF3, we examined whether TRAF3 is targeted for ubiquitin-mediated proteasomal degradation by UBR5, as UBR5 belongs to the HECT-type E3 ubiquitin ligase family (8). To block the ubiquitin-mediated proteasomal degradation pathway and assess the TRAF3 level, MG132, a proteasome inhibitor, was used in the stable cell lines expressing control or UBR5 shRNA. MG132 treatment, however, did not make any significant difference in the TRAF3 level in either of the cell lines (Fig. 2*A*). Autophagy is another protein degradation system that recog-

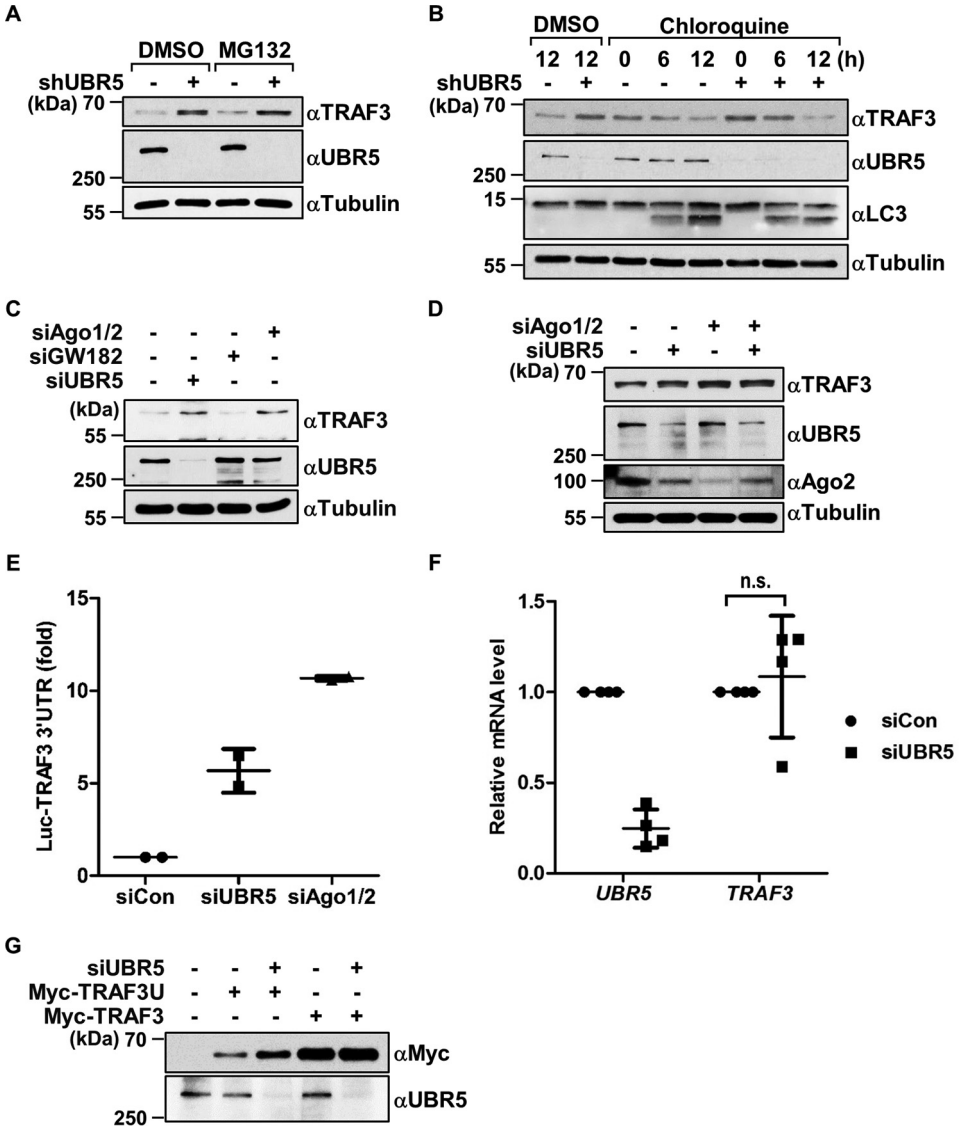

Figure 2. UBR5 regulates TRAF3 expression through miRNA-mediated translational repression. *A* and *B*, immunoblot analysis of the indicated proteins using the whole-cell lysates of HeLa cell lines stably expressing control or UBR5 shRNA treated with DMSO or MG132 (10 μM) for 6 h (*A*) or with chloroquine (100 nM) for the indicated time periods (*B*). *C* and *D*, immunoblot analysis of the indicated proteins using the whole-cell lysates of HeLa cells transfected with siRNAs against Ago1/2, GW182, UBR5, or control siRNA for 72 h. *E*, luciferase assay of TRAF3 3′-UTR luciferase activity using lysate of HeLa cells that were transfected with siRNAs against UBR5, Ago1 or -2, or control siRNA. Data are shown as the mean ± S.D. of duplicate samples from a representative experiment performed three times. *F*, qPCR analysis of *UBR5* and *TRAF3* mRNA level in control and UBR5 siRNA–transfected HeLa cells. Data are shown as the mean ± S.D. of duplicate samples from a representative experiment performed three times (*n.s.* (non-significant), Student's *t* test). *G*, immunoblot analysis of exogenous Myc-tagged TRAF3 containing the 3′-UTR region (Myc–TRAF3U) or not (Myc–TRAF3) in HeLa cells that were transfected with control or UBR5 siRNA for 72 h. Data are representative of at least two independent experiments.

nizes the ubiquitinated proteins and degrades them by the lysosomal degradation pathway (25). Chloroquine, a lysosomal degradation inhibitor, also failed to raise the level of TRAF3; it even decreased the amount of TRAF3 while successfully blocking the degradation of LC3 proteins by autophagy (Fig. 2*B*). Together, these results suggest that UBR5 activity does not result in a decrease in the TRAF3 protein level via proteasome or lysosome.

Alternatively, it has been reported that UBR5 is involved in the miRNA-mediated gene-silencing pathway (26). A study by H. Su *et al.* (26) suggested that UBR5 interacts directly with GW182, leading to miRNA-mediated gene silencing without affecting miRNA biogenesis. To examine whether TRAF3 is regulated through the same pathway, we attempted to inhibit assembly of miRISC by depleting the key component proteins of miRISC such as Argonaute (Ago1 and Ago2) and GW182 (TNRC6A) in HeLa cells (supplemental Fig. 2, *A–D*). Simultaneous knockdown of Ago1 and Ago2 resulted in increased TRAF3 level similar to that of knockdown of UBR5 (Fig. 2*C*). Moreover, the effect of the knockdown of both UBR5 and Ago1/2 was not additive for the TRAF3 level (Fig. 2*D*), suggesting that UBR5 and Ago are on the same signaling pathway to control TRAF3 and that the expression of TRAF3 is regulated by the miRNA pathway. However, knockdown of TNRC6A failed to increase the amount of TRAF3 proteins. In mammals, the GW182 protein family has three paralogues, named TNRC6A, -B, and -C. Because these paralogues have redundant functions in the miRNA pathway, the depletion of TNRC6A

ASBMB

alone may not be enough to inhibit the assembly of miRISC and the general miRNA pathway (27). To further investigate whether UBR5 regulates TRAF3 through the miRNA-mediated gene-silencing pathway, we generated the firefly (*Photinus pyralis*) luciferase reporter plasmid (Luc–TRAF3 3′-UTR) in which the 5′-proximal part of the 3′-UTR of TRAF3 is attached to the 3′-end of the firefly luciferase gene. This 3′-UTR sequence (1313 bp) contains two previously reported target sites of miRNA, miR32(461–467) (28) and miR422(1134–1140) (29). The expression of firefly luciferase is driven by the CMV promoter and supposedly suppressed by cellular miRNAs. Depletion of either UBR5 or Ago1/2 in HeLa cells significantly increased the activity of the Luc–TRAF3 3′-UTR reporter, strongly suggesting that UBR5 is involved in the miRNA pathway (Fig. 2*E*). Additionally, no significant change in the abundance of TRAF3 mRNA was observed in UBR5 knockdown cells, indicating that miRNA-induced mRNA degradation is not involved in the regulation of the TRAF3 level by UBR5 (Fig. 2*F*). To further confirm the miRNA-mediated regulation of TRAF3 by UBR5, the expression of a Myc–TRAF3 3′-UTR construct was compared with that of a Myc–TRAF3 construct containing only the coding sequence. In agreement with the luciferase reporter data, the expression of Myc–TRAF3 3′-UTR was elevated by UBR5 siRNA, but that of Myc-TRAF3 was not (Fig. 2*G*). Together, these data suggest that UBR5 regulates TRAF3 expression through miRNA-mediated translational repression.

RSK phosphorylates UBR5 at Ser^{2483}

In an attempt to identify the upstream regulators of UBR5 involved in miRNA-mediated TRAF3 regulation, we performed a post-translational modification (PTM) database search with PhosphoSite Plus (www.phosphosite.org)[5] (30) to define the PTMs that occur in UBR5. Among 114 potential phosphorylation sites (supplemental Table 1), we noted that Ser^{2483} of UBR5 belongs to the typical consensus motif (Arg-*X*-Arg-*X*-*X*-Ser/Thr, where *X* is any amino acid) that is preferentially phosphorylated by AGC kinases, including Akt, p70 ribosomal S6 kinase (S6K), serum and glucocorticoid-regulated kinase (SGK), and p90RSK (31); this motif is evolutionarily conserved in vertebrates (Fig. 3*A*). To confirm the phosphorylation of UBR5 at Ser^{2483}, we used the anti-R*X*R*XX*p(S/T) antibody, which has been used for the identification of the substrates of AGC kinases. After the FLAG-wild type UBR5 and -Ser^{2483}Ala (SA) and -Ser^{2483}Glu (SE) mutant UBR5 were transfected in COS-1 cells, the phosphorylation status of the immunoprecipitated exogenous UBR5 was examined using the anti-R*X*R*XX*p(S/T) antibody. Although the SE and SA mutants of UBR5 were not detected by the phospho-antibody, wild-type UBR5 was recognized (Fig. 3*B*). Akt, S6K, SGK, and p90RSK are activated downstream of extracellular growth factor stimuli by the PI3K–mTOR or the Ras–ERK pathway (31). Indeed, treatment with EGF, phorbol 12-myristate 13-acetate (PMA), or fetal bovine serum (FBS) induced the phosphorylation of UBR5 in serum-starved HeLa cells (Fig. 3*C*). It was also demonstrated that the phosphorylation level at Ser^{2483} of UBR5 reached a peak at 15 min after stimulation with EGF in COS-1 and HEK293T cells (supplemental Fig. 3, *A* and *B*, respectively). To determine which kinase was responsible for the Ser^{2483} phosphorylation of UBR5, we used two specific inhibitors: GDC0349, an mTOR kinase inhibitor that blocks the activation of Akt, S6K, and SGK; and BI-D1870, a p90RSK inhibitor. As a result, treatment with BI-D1870 completely inhibited the UBR5 phosphorylation induced by EGF stimulation compared with GDC0349 (Fig. 3*D*). To confirm the results at the endogenous level, the antibody which specifically recognizes Ser^{2483}-phosphorylated UBR5 was raised and used to examine the phosphorylation of endogenous UBR5. The specificity of the antibody was validated by a dot blot assay and immunoblot analysis (supplemental Fig. 3, *C* and *D*, respectively). Using this anti-phospho-Ser^{2483} UBR5 antibody (anti-pUBR5 antibody), we observed that the endogenous UBR5 was able to be phosphorylated by EGF, poly(I:C), and LPS stimulation and that treatment with BI-D1870 successfully diminished the phosphorylation (Fig. 3*E* and supplemental Fig. 3, *E* and *F*, respectively). Phosphorylation of UBR5 following poly(I:C) treatment is weaker than that induced by LPS (supplemental Fig. 3, *E* and *F*), suggesting that the p90RSK–UBR5 pathway might be affected differentially by viral and bacterial infection.

Next, to examine the possibility that p90RSK directly phosphorylates UBR5, we assessed UBR5 phosphorylation in p90RSK1/2/3-depleted COS-1 cells. Simultaneous knockdown of p90RSK1/2/3 by siRNA in COS-1 cells significantly attenuated Ser^{2483} phosphorylation of UBR5 (Fig. 3*F*). The overexpression of p90RSK in COS-1 cells induced the Ser^{2483} phosphorylation (Fig. 3*G*). Furthermore, through co-immunoprecipitation analysis, p90RSK was found to interact with UBR5 in HEK293T cells (Fig. 3*H*). Finally, an *in vitro* kinase assay using FLAG–wild-type UBR5 or SA mutant UBR5 as a substrate showed that immunoprecipitated Myc–p90RSK was able to phosphorylate wild-type UBR5 proteins but phosphorylate mutant UBR5 to a lesser extent (Fig. 3*I*). These results suggest that there are other phosphorylation sites of p90RSK in UBR5. Of the sites registered to be phosphorylated, Ser^{2483} is the only residue bearing the R*X*R*XX*(S/T) motif. Instead, there are two more putative p90RSK consensus sites, Thr^{637} and Ser^{1227}, containing basic residues in the -3 and -5 region ((K/R)*X*(K/R)*XX*(S/T)) (31). Thr^{637} and Ser^{1227} are located in the K*X*R*XX*T and K*X*K*XX*S motifs, respectively, and conserved throughout vertebrates (supplemental Fig. 3, *G* and *H*). In an *in vitro* kinase assay using UBR5 and p90RSK, the T637A or S1227A mutation in UBR5 also resulted in the reduction of the p90RSK-mediated phosphorylation of UBR5 (Fig. 3*J*). Moreover, a UBR5 mutant, in which all three residues were replaced with Ala (3A), was less phosphorylated by p90RSK than the UBR5 SA mutant (Fig. 3*K*). These data suggested that p90RSK directly phosphorylates UBR5 at Thr^{637}, Ser^{1227}, and Ser^{2483}.

p90RSK negatively regulates TRAF3–TBK1 signaling by phosphorylating UBR5

The inhibition of p90RSK activity with BI-D1870 or siRNAs targeting p90RSK1, -2, and -3 in HeLa cells resulted

[5] Please note that the JBC is not responsible for the long-term archiving and maintenance of this site or any other third party hosted site.

in a substantial increase in the TRAF3 level and phosphorylation of TBK1 in the absence of any exogenous stimulation (Fig. 4, *A* and *B*), indicating that p90RSK activity is required for the repression of the TRAF3 level and TBK1 activity as in the case of UBR5. Moreover, BI-D1870 treatment induced IFNβ mRNA (Fig. 4*C*), and knockdown of p90RSK increased the activity of the TRAF3 3′-UTR reporter (Fig. 4*D*). Furthermore, the exogenous expression of constitutively active p90RSK (RSK CA) (32) reduced the expression of the TRAF3 3′-UTR construct (Fig. 4*E*). Finally, the effects of BI-D1870 treatment and UBR5 knockdown were not additive at the TRAF3 level, indicating that p90RSK and UBR5 may be on the same signaling pathway (Fig. 4, *F* and *G*).

p90RSK–UBR5 pathway regulates KRAS and p60 katanin expression

It has been demonstrated that *let-7* miRNA-mediated gene silencing is compromised in UBR5-depleted HeLa cells, which leads to an increase in the expression of HMGA2, a *let-7* miRNA target gene (26). We confirmed that the activity of the

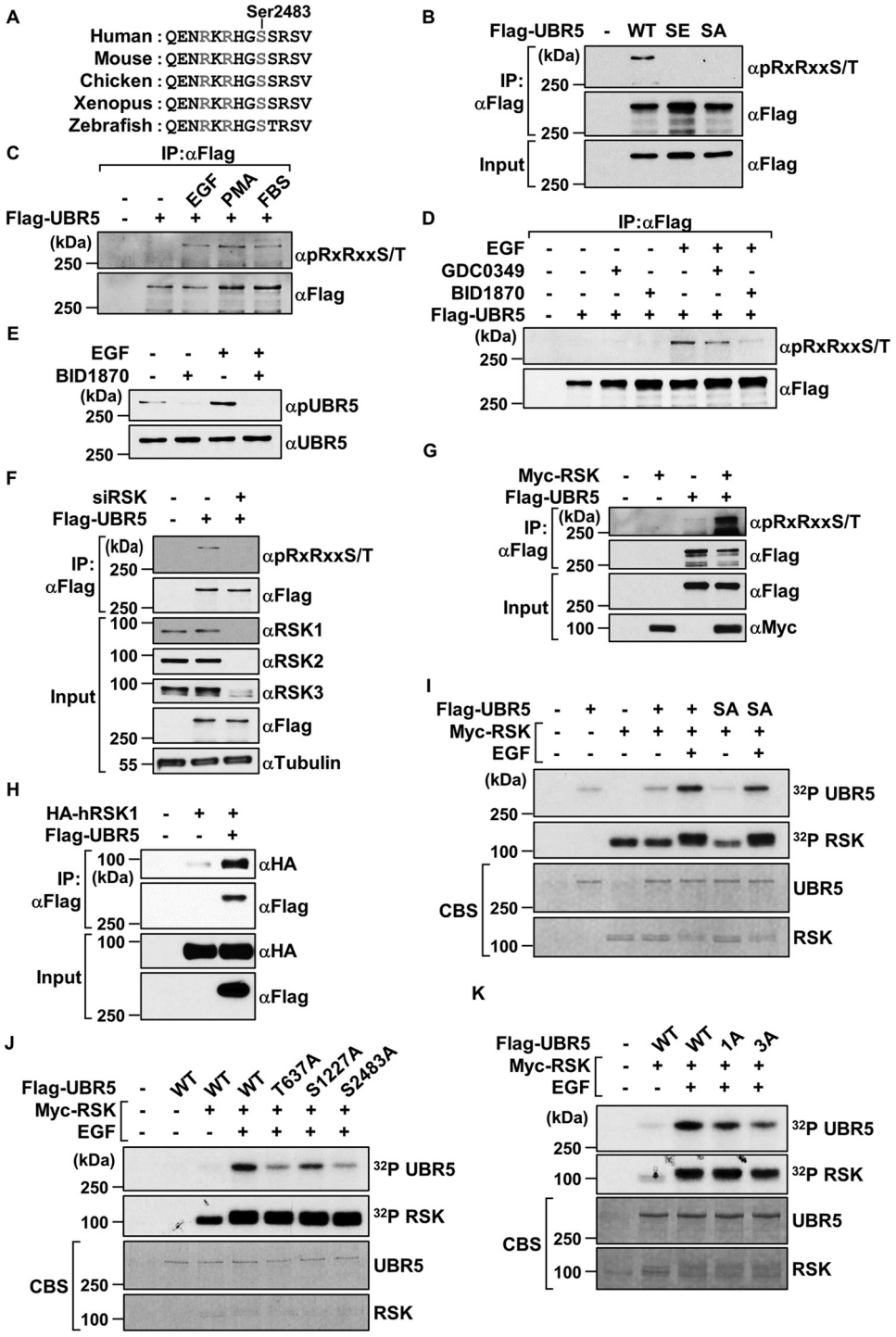

firefly luciferase reporter plasmid (Luc-KRAS 3′-UTR), in which 3′-UTR of KRAS is attached to the 3′-end of the firefly luciferase gene (33), was indeed increased by the knockdown of UBR5 (Fig. 5*A*) and decreased by the overexpression of UBR5 (Fig. 5*G*). Next, the inhibition of p90RSK activity by BI-D1870 or depletion of p90RSK via RNA interference resulted in a significant increase in Luc–KRAS 3′-UTR activity (Fig. 5, *B* and *C*, respectively). In addition, overexpression of RSK CA in HeLa cells significantly decreased Luc–KRAS 3′-UTR activity (Fig. 5*D*). These data suggest that the regulation of miRNA-mediated gene silencing by the p90RSK–UBR5 pathway may be a general phenomenon.

To find other target proteins that are controlled by the p90RSK–UBR5 pathway, we tested whether p90RSK could regulate proteins known to be controlled by UBR5. p60 katanin, a microtubule-associated AAA-ATPase, is known as one of the substrates for the UBR5–DYRK2–DDB1–VPRBP E3 ligase complex (13). In agreement with the previous result, p60 katanin was found to be increased in UBR5-depleted HeLa cells (supplemental Fig. 4*A*). Surprisingly, the treatment of BI-D1870 or siRNA transfection of p90RSK in HeLa cells resulted in increase in the p60 katanin protein level (supplemental Fig. 4, *B* and *C*). These data suggested the possibility that the abundance of p60 katanin protein may be controlled through the p90RSK–UBR5 pathway–regulated miRNA pathway as well as the UBR5–DYRK2–DDB1–VPRBP E3 complex.

miRISCs have been localized mainly in cytoplasmic processing bodies (34), whereas UBR5 has also been known to be localized in the nucleus (9). To resolve this discrepancy, we examined the localization of UBR5 and p90RSK by cell fractionation. Both UBR5 and p90RSK were found in the cytoplasm as well as the nucleus, and the phosphorylation of UBR5 was elevated by EGF treatment and down-regulated by BI-D1870 treatment (supplemental Fig. 5, *A* and *B*). In addition, both the anti-UBR5 and anti-pUBR5 antibodies strongly stained the nucleus, and prominent cytoplasmic speckles or puncta were also shown by anti-pUBR5 antibody (supplemental Fig. 5*C*). To examine the specificity of the antibody, the peptides used for raising the antibody were added to the cells, abrogating the cytoplasmic puncta and the nuclear staining (supplemental Fig. 5*C*). It did not seem, however, that Ser^{2483} phosphorylation of UBR5 induce the nuclear cytoplasmic shuttling of UBR5 (supplemental Fig. 5, *A* and *B*). Furthermore, some of these intriguing speckles colocalized with GW182 and Ago2, which are the components of miRISCs in the cytoplasm, and the colocalization signals were decreased following treatment with BI-D1870 (supplemental Fig. 5, *D–G*). These data suggest that the cytoplasmic p90RSK–UBR5 pathway regulates miRNA-mediated gene silencing.

To further investigate the roles of p90RSK-mediated UBR5 phosphorylation in the miRNA pathway, we assessed the interaction between GW182 or Ago2 and the phosphorylated UBR5. The phosphomimic UBR5 mutant with the substitution of Glu for Thr^{637}/Ser^{1227}/Ser^{2483} (3E) associated more tightly with GW182 and Ago2 than wild-type UBR5, but the interaction of UBR5 3SA mutant with GW182 and Ago2 was decreased (Fig. 5, *E* and *F*). In agreement with these results, the UBR5 3E mutant further decreased Luc–KRAS 3′-UTR activity in comparison with wild-type UBR5 in UBR5-depleted HEK293 cells, but the UBR5 3A mutant did not (Fig. 5*G* and supplemental Fig. 4*D*). Together these results suggested that phosphorylation of UBR5 at Thr^{637}, Ser^{1227}, and Ser^{2483} by p90RSK was required for miRNA-mediated gene silencing.

Discussion

In a recent study, UBR5 was suggested as a substrate of a deubiquitinating enzyme DUBA (also known as OTUD5) (19). DUBA has been first identified as a negative regulator of TRAF3 in TLR signaling (20). Upon the activation of TLR, DUBA is subsequently activated (35) and negatively regulates the induction of type I Interferon by removing the Lys^{63}-linked ubiquitin chain of TRAF3 (20). DUBA stability is regulated by E3 ubiquitin ligase UBR5 (19) as well as its deubiquitinase activity (35). The question that UBR5 regulates the TLR-mediated TRAF3 signaling via DUBA was raised. Knockdown of UBR5, however, resulted in the increase of TRAF3 proteins, activation of TBK1, and production of IFNβ despite the substantial increase of DUBA (Fig. 1). Furthermore, the amount of TRAF3 was controlled by UBR5-regulated miRNA pathway (Fig. 2). These data strongly suggested that DUBA and UBR5 converge on TRAF3 signaling in parallel, independently of the DUBA–UBR5 axis presented in the previous study (19).

TLRs activates mitogen-activated protein kinase (MAPK) pathway, including ERK, JNK, and p38, to induce the genes encoding inflammatory cytokines and generate immune

Figure 3. p90RSK phosphorylates UBR5 at multiple sites. *A*, conservation of R*X*R*XX*S motif of UBR5 Ser^{2483} among various species. *B*, FLAG–wild-type UBR5 (WT) or the indicated UBR5 mutant (S2483A (SA) and S2483E (SE)) were transfected in COS-1 cells. The FLAG–UBR5 proteins were isolated by immunoprecipitation and subjected to immunoblot analysis for phosphorylation using the indicated antibodies (*top* and *middle panels*). The cell lysates were subjected to direct immunoblot (*bottom panel*, Input = 2% of the total lysates). *C*, after 24-h serum starvation, the HeLa cells transfected with FLAG–UBR5 were stimulated with EGF (100 ng/ml), PMA (50 ng/ml), or FBS (20%) for 15 min. The lysates were subjected to immunoprecipitation followed by immunoblot analysis using the indicated antibodies. *D*, after 24-h serum starvation, the COS-1 cells were pretreated with GDC0349 (1 μM) or BI-D1870 (10 μM) for 30 min prior to EGF (100 ng/ml) stimulation for 15 min. The FLAG–UBR5 proteins were isolated by immunoprecipitation and subjected to immunoblot analysis using the indicated antibodies. *E*, the serum-starved COS-1 cells were stimulated with EGF for 15 min in the absence or presence of BI-D1870 (for 30 min). The cell lysates were subjected to immunoblot analysis using the indicated antibodies. *F*, COS-1 cells were transfected with control siRNA or p90RSK1, -2, or -3 siRNA and empty vector or FLAG–UBR5 as indicated. The FLAG–UBR5 proteins were isolated by immunoprecipitation and subjected to immunoblot analysis using the indicated antibodies (*IP*), and the cell lysates were subjected to direct immunoblot with the indicated antibodies (*Input*). *G*, COS-1 cells were cotransfected with empty vector or Myc–avian p90RSK and empty vector or FLAG–UBR5 as indicated. The FLAG–UBR5 proteins were isolated by immunoprecipitation and subjected to immunoblot analysis using indicated antibodies (*IP*), and the cell lysates were subjected to direct immunoblot with the indicated antibodies (*Input*). *H*, COS-1 cells were cotransfected with empty vector or HA–human p90RSK1 (*hRSK1*) and empty vector or FLAG–UBR5 as indicated. The FLAG–UBR5 proteins were isolated by immunoprecipitation and subjected to immunoblot analysis with the indicated antibodies to detect UBR5–p90RSK1 interaction (*IP*), and the cell lysates were subjected to direct immunoblot with the same antibodies (*Input*). *I–K*, *in vitro* kinase assay using FLAG–UBR5 and Myc–avian p90RSK (*I*), FLAG-WT-UBR5, FLAG-T637A-UBR5, FLAG-S2483A-UBR5, and Myc–avian p90RSK (*J*), FLAG-WT-UBR5, FLAG-S2483A-UBR5 (*1A*), T637/S1227/S2483A-UBR5 (*3A*), and Myc–avian p90RSK (*K*) as described under "Experimental procedures." *CBS*, Coomassie Blue staining.

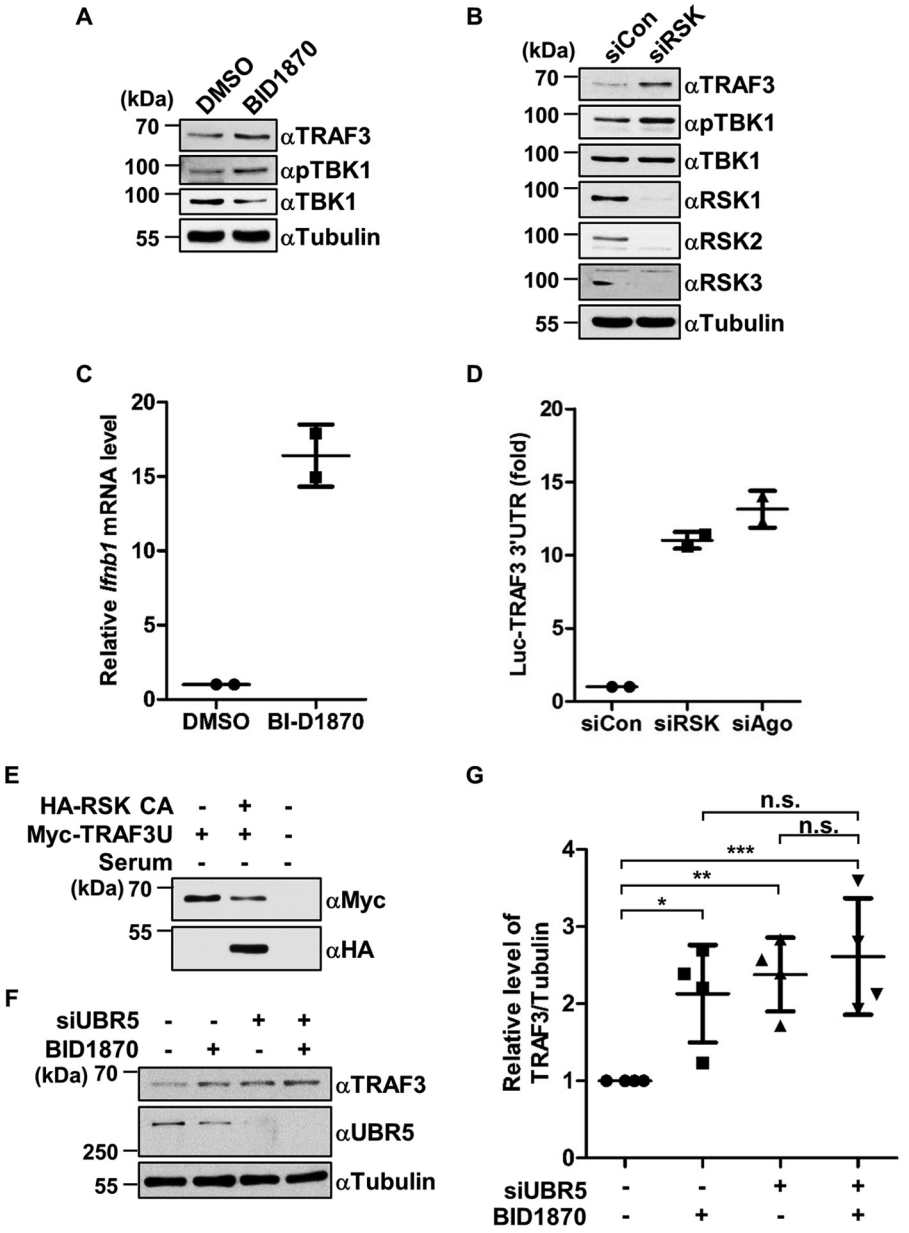

Figure 4. p90RSK negatively regulates TRAF3–TBK1 signaling via UBR5. *A* and *B*, immunoblot analysis of the indicated proteins using the whole-cell lysates of HeLa cells that were treated with DMSO or BI-D1870 for 12 h (*A*) or transfected with siRNAs against p90RSK1/2/3 and control siRNA for 48 h (*B*). All of the immunoblots were completed using the same cell lysates. *C*, qPCR analysis of *Ifnb1* mRNA level using HeLa cells treated with DMSO or BI-D1870 for 12 h. Data are shown as the mean ± S.D. of duplicate samples from a representative experiment performed three times. *D*, Dual-Luciferase assays were performed using a TRAF3 3′-UTR reporter in HeLa cells transfected with siRNAs against p90RSK1/2/3, Ago-1 and -2, and control siRNA. Data are shown as the mean ± S.D. of duplicate samples from a representative experiment performed three times. *E*, HeLa cells were cotransfected with empty vector or Myc-TRAF3U and empty vector or HA–human RSK CA as indicated for 48 h. After a 12-h serum starvation, the cell lysates were subjected to immunoblot analysis with the indicated antibodies. *F*, immunoblot analysis of indicated proteins using DMSO or BI-D1870 (for 12 h) treated HeLa cells transfected with siRNAs against control or UBR5 for 48 h. *G*, densitometry analysis of immunoblot bands from *F* from four independent experiments. TRAF3 bands were normalized to tubulin bands. Data are shown as the mean ± S.D. from four independent experiments (*, $p = 0.005$; **, $p = 0.0005$; ***, $p = 0.002$; and *n.s.* (non-significant), Student's *t* test).

responses (36). In macrophages and myeloid dendritic cells, it was reported that TPL2-mediated ERK activation negatively regulates IFNβ production (37). It is very well known that p90RSK is directly phosphorylated and activated by ERK (38), however, the functions and substrates of p90RSK in immune response remain elusive (36). In present study, we found that the p90RSK directly phosphorylates UBR5 at Thr^{637}, Ser^{1227}, and Ser^{2483} in response to the activation of TLRs as well as EGF receptor (Fig. 3 and supplemental Fig. 3) and the inhibition of UBR5 phosphorylation abolished the translational repression of TRAF3 and KRAS repression (Figs. 4 and 5). In terms of TLR signaling, these results propose the possibility that pathogen-associated molecular patterns may activate the TRAF3–TBK1 pathway via Lys^{63} ubiquitination, as well as fine-tuning the strength of the signaling via p90RSK–UBR5 pathway-mediated suppression of TRAF3 expression and DUBA-mediated deubiquitination of TRAF3. The miRNA pathway can be regulated through controlling the activity of miRISC as well as biogenesis of miRNAs (39). To date, a number of upstream regulators and PTMs of Ago protein have been iden-

ASBMB

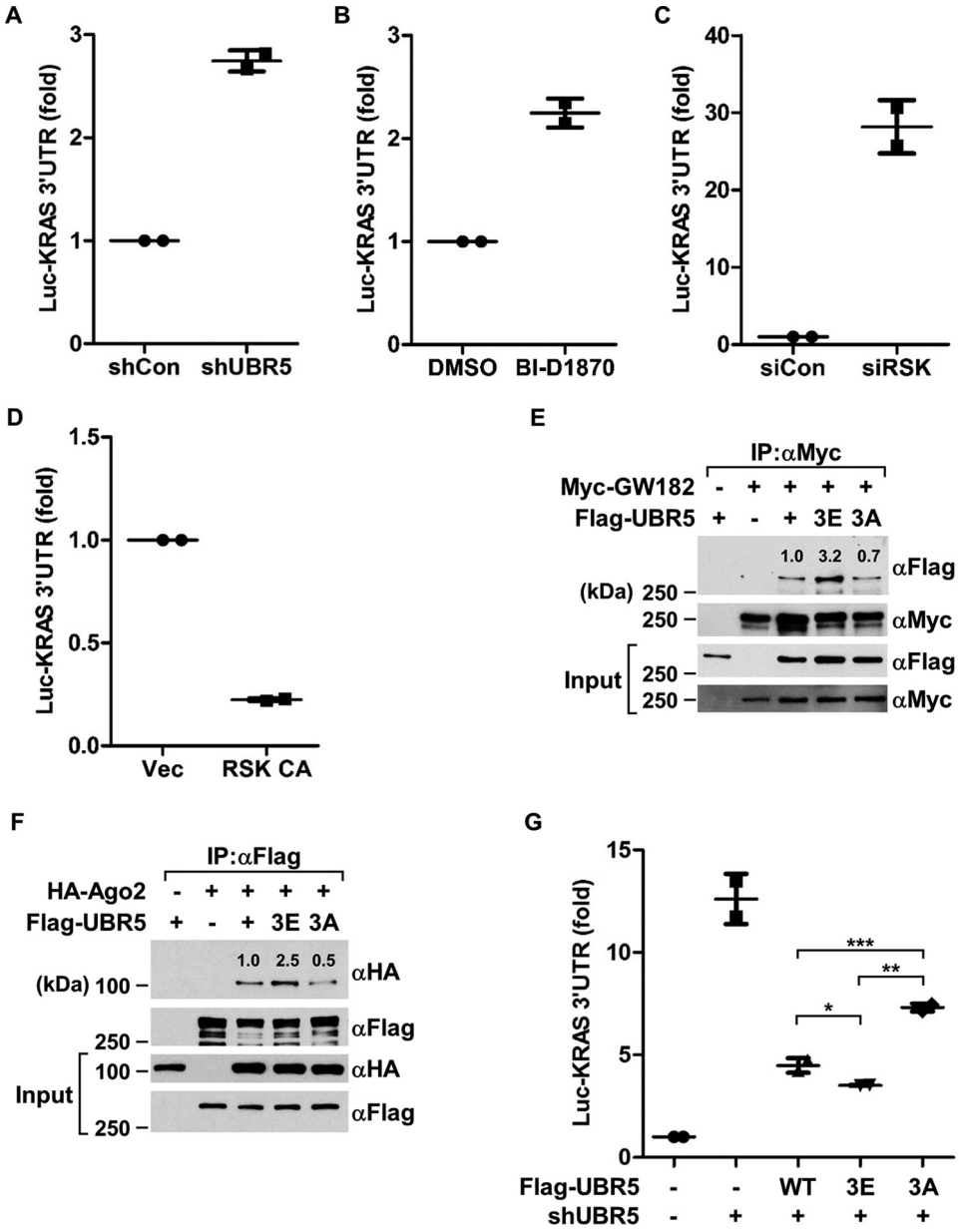

Figure 5. p90RSK–UBR5 pathway regulates KRAS and p60 katanin expression. *A*, Dual-Luciferase assays using a KRAS 3′-UTR reporter were carried out using the whole-cell lysates of control or UBR5 shRNA stable HeLa cells. Data are shown as the mean ± S.D. of duplicate samples from a representative experiment performed three times. *B–D*, KRAS 3′-UTR reporter assays were performed using the cells treated with DMSO or BI-D1870 for 12 h (*B*), transfected with control or p90RSK1, -2, and -3 siRNAs for 48 h (*C*), or transfected with empty vector or HA–RSK CA for 48 h (*D*). Data are shown as the mean ± S.D. of duplicate samples from a representative experiment performed two times. *E*, HEK293 cells were cotransfected with empty vector (−) or FLAG–wild type (+), 3E, or 3A mutant UBR5 and Myc–GFP–GW182 as indicated. After 48 h, the Myc–GFP–GW182 cells were immunoprecipitated using anti-Myc antibody and subjected to immunoblot analysis with the indicated antibodies to detect UBR5 and GW182 interaction (*IP*), and the cell lysates were subjected to direct immunoblot with same antibodies (*Input*). *F*, HEK293 cells were cotransfected with empty vector (−) or FLAG–wild type(+), 3E, or 3A mutant UBR5 and HA–Ago2 as indicated. After 48 h, the FLAG–UBR5 proteins were immunoprecipitated using anti-FLAG antibody and subjected to immunoblot analysis with the indicated antibodies to detect UBR5 and Ago2 interaction (*IP*), and the cell lysates were subjected to direct immunoblot with same antibodies (*Input*). *G*, luciferase assay of KRAS 3′-UTR luciferase activity using control or UBR5 shRNA stable HEK293 cell lysates cotransfected with Luc–KRAS 3′-UTR, pRL-CMV, and empty vector (−), FLAG–WT UBR5, 3E, or 3A mutant. Data are shown as the mean ± S.D. of duplicate samples from a representative experiment performed twice. (*, $p = 0.03$; **, $p = 0.0006$; ***, $p = 0.005$; Student's *t* test).

tified. PTMs of Ago protein, including phosphorylation, hydroxylation, ubiquitination, altered the stability, ability of binding to small RNA molecules, and cellular localization of Ago (40–43). In the present study, we suggested another regulator mechanism for regulating miRISC activity by phosphorylating UBR5 (Fig. 6).

UBR5 3A mutants are still able to be phosphorylated by activated p90RSK in *in vitro* kinase assay (Fig. 3*K*). This result raised the possibility that there are other phosphorylation sites in UBR5. There are two evolutionarily conserved R*X*R*XX*(S/T) motifs in human UBR5, Ser^{26} and Ser^{2483}. Phospho-R*X*R*XX*(S/T) antibody, however, did not recognize the Ser^{2483} mutants of UBR5 (Fig. 3*B*), indicating that Ser^{26} is barely phosphorylated by p90RSK. Although there may be more phosphorylation sites of UBR5 by p90RSK, it has been shown that 3E mutant interacts with GW182 and Ago2 stronger

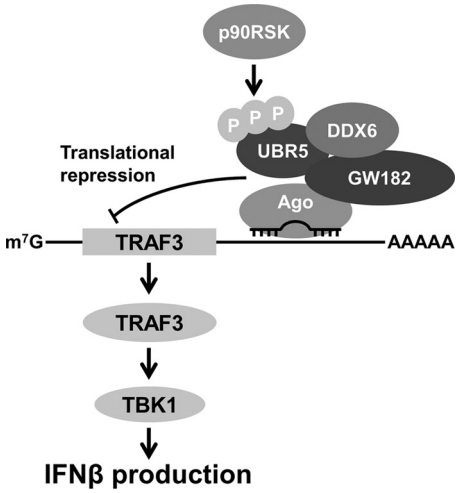

Figure 6. Schematic overview of p90RSK-mediated regulation of UBR5-containing miRISC.

than wild-type and 3A mutant is weaker than wild-type and 3E mutant in terms of the association with miRISC and translational repression (Fig. 5, *E–G*). These data collectively suggest that three residues are the main regulatory sites in UBR5.

UBR5 proteins have been shown to reside in the nucleus (9). In contrast, miRISCs are localized mainly in cytoplasmic processing bodies (34). The nuclear cytoplasmic fractionation and immunocytochemistry showed that a part of phosphorylated UBR5 is colocalized with a subset of miRISC proteins at the cytoplasmic punctate structure (supplemental Fig. 5). These findings suggest the possibility that there are UBR5-specific miRISC sets. Further study will be needed to elucidate the components of the p90RSK–UBR5– containing miRISCs and their target miRNA-mRNA sets.

Together our findings have established p90RSK–UBR5 pathway as a positive regulator of miRNA-mediated gene silencing pathway and a negative regulatory mechanism of TLR signaling.

Experimental procedures

Antibodies and reagents

Anti-UBR5 antibody (#8755), TRAF3 antibody (#4729), TBK1 antibody (#3504), phospho-TBK1 Ser^{172} antibody (#5483), phospho-Akt substrate (RXRXXp(S/T)) antibody (#10001), RSK1 antibody (#8408), and RSK2 antibody (#5528) were obtained from Cell Signaling Technology. Anti-DUBA antibody (ab176727), GW182 antibody (ab70522), and Ago2 antibody (ab57113) were obtained from Abcam. Anti-RSK3 antibody (sc1431), DDX6 antibody (sc376433), and Myc antibody (sc40) were obtained from Santa Cruz Biotechnology. Anti-LC3 antibody (PM036) was obtained from MBL. Anti-HA antibody (#11867423001) was obtained from Roche Life Science. Anti-FLAG antibody (F1804) and tubulin antibody (T5168) were obtained from Sigma-Aldrich. Polyclonal anti-phospho-UBR5 Ser^{2483} antibody was developed in rabbits using a synthetic phosphopeptide derived from 2476–2486 amino acids of human UBR5 as an immunogen, and the serum was purified by affinity chromatography by AbClon (Seoul, Republic of Korea). Anti-FLAG M2 affinity gel (A2220) and anti-c-Myc-agarose gel (A7470) were obtained from Sigma-Aldrich. Protein G-Sepharose (#17-0618-01) was obtained from GE Healthcare. MG132 (C2211), chloroquine (C6628), EGF (E9644), PMA (P1585), and polyinosinic-polycytidylic acid potassium salt (poly(I:C), I3036) were obtained from Sigma-Aldrich. BI-D1870 (S2843) and GDC0349 (S8040) were obtained from Selleck Chemicals.

Cell culture

HeLa, COS-1, and HEK293T cells were maintained in Dulbecco's modified Eagle's medium (DMEM, Gibco) supplemented with 10% FBS (Gibco), 100 units/ml penicillin, 100 μg/ml streptomycin, and 0.25 μg/ml amphotericin B (Gibco) in a humidified atmosphere of 5% CO_2 in air at 37 °C.

Plasmids and transfection

Myc-GFP-TNRC6A (#41999) and GFP-hAgo2 (#11590) were obtained from Addgene. Cells were transfected with various plasmids using X-tremeGENE HP DNA transfection reagent (Roche Life Science) according to the manufacturer's instruction.

RNA interference

siRNA against Ago1 (siRNA no.1046447), Ago2 (siRNA no.1046457), TNRC6A (siRNA no.1154883), and negative control siRNA (SN-1003) were obtained from Bioneer (Daejeon, Republic of Korea). siRNA against DUBA (L-013823-00) was obtained from Dharmacon. siRNA against UBR5 was obtained from Santa Cruz Biotechnology (sc-43744) and Bioneer (siRNA no. 1045520). siRNA against RSK1, -2, and -3 were obtained from Dharmacon (L-003025-00, L-003026, and L-004663-00) and Bioneer (siRNA no.1131587, 1131617, and 1131598). For RNA interference, cells were transfected with various siRNA using Lipofectamine RNAiMAX transfection reagent (Invitrogen) according to the manufacturer's instruction. After 48–72 h of incubation, the cells were harvested and analyzed.

Lentivirus production and transduction

For production of lentiviral particles, HEK293T cells were transfected with the lentiviral plasmid pLKO.1 containing UBR5 3′-UTR targeting shRNA (TRCN0000226459, Sigma-Aldrich) or non-targeting shRNA (SHC202, Sigma-Aldrich), psPAX2, and pMD2.G at a ratio of 1:0.75:0.25. After 72 h of transfection, supernatants containing lentiviruses were collected and filtered through a 0.45-μm sterile filter to remove cell debris. To generate stably expressed UBR5 or negative control shRNA HeLa cells, cells were treated with the viral supernatant and 8 μg/ml hexadimethrine bromide (H9268, Sigma-Aldrich) and incubated for 48 h. After viral transduction, cells were treated and selected with 2 μg/ml puromycin.

Immunoprecipitation and immunoblotting

Cells were lysed using lysis buffer (50 mM HEPES–KOH, pH 7.4, 40 mM NaCl, 1 mM EDTA, 1 mM EGTA, 10 mM sodium pyrophosphate, 10 mM sodium β-glycerophosphate, 50 mM NaF, 1 mM $NaVO_4$, and 1% Triton X-100) containing protease inhibitor (#05056489001, Roche Life Science). The lysate was

ASBMB

clarified by centrifuging at 13,000 rpm and 4 °C for 15 min. The supernatant was quantified and incubated with antibodies and beads at 4 °C for 2 h or overnight. After incubation, the beads were washed twice in lysis buffer, twice in wash buffer (50 mM HEPES–KOH, pH 7.4, 500 mM NaCl, 1 mM EDTA, 1 mM EGTA, 10 mM sodium pyrophosphate, 10 mM sodium β-glycerophosphate, 50 mM NaF, 1 mM $NaVO_4$, 1% Triton X-100, and protease inhibitor), and once in lysis buffer. In co-immunoprecipitation experiments, the beads were washed three times in lysis buffer. Elution was performed using 2× Laemmli buffer, and samples were separated using SDS-PAGE. After transfer to nitrocellulose membrane, immunoblotting was performed using the indicated antibodies.

Luciferase assay

HeLa cells were transfected with the indicated siRNAs. After a 24-h transfection, then cells were transfected with the indicated luciferase reporter plasmids and pRL-CMV for 48 h. Luciferase activities were measured using the Dual-Luciferase reporter assay system (Promega) according to the manufacturer's instruction.

Real-time PCR analysis

Total RNA was extracted from siRNA- or chemical-treated cells using the RNeasy Plus mini kit (Qiagen), and 2 μg of total RNA was reverse-transcribed using the RevertAid H Minus first-strand cDNA synthesis kit (Thermo Fisher Scientific) according to the manufacturer's instruction. Real-time PCR was performed using Solg 2× Real-time PCR Smart mix (SRH71-M40H, SolGent Co.) and gene-specific primers. Human *GAPDH* gene was used for normalization. The sequence of primers used for real-time PCR is shown in supplemental Table 2.

In vitro kinase assay

HEK293 cells were transfected with plasmids encoding FLAG-tagged wild-type and mutant UBR5 and Myc-tagged avian RSK, respectively. After a 48-h transfection, FLAG–UBR5 overexpressed cells were serum-starved for 24 h and then treated with 10 μM BI-D1870 for 5 h. Myc-RSK overexpressed cells were serum-starved for 24 h and then stimulated with 100 ng/ml EGF (or not, as indicated) for 30 min. Cells were rinsed with ice-cold PBS and lysed using lysis buffer. The clarified lysates were immunoprecipitated with anti-FLAG–agarose gel (for FLAG–UBR5) or anti-c-Myc–agarose gel (for Myc-RSK) at 4 °C for 3 h. The beads were washed twice in lysis buffer, twice in wash buffer, once in lysis buffer, and once in kinase buffer (25 mM HEPES-KOH, pH 7.4, 10 mM $MgCl_2$, 3 mM β-mercaptoethanol, 0.1 mg/ml BSA, and 1 mM DTT). In the last washing step, FLAG–UBR5 (or negative control)–bound beads and Myc-RSK (either stimulated or not with EGF)–bound beads were combined as indicated. The kinase assay was performed by adding kinase reaction buffer (25 mM HEPES–KOH, pH 7.4, 10 mM $MgCl_2$, 3 mM β-mercaptoethanol, 0.1 mg/ml BSA, 1 mM DTT, 50 μM ATP, and 10 μCi of [γ-^{32}P]ATP) and incubating at 30 °C for 30 min. Reactions were stopped by adding Laemmli buffer and boiling at 100 °C for 5 min. The proteins were separated using SDS-PAGE, and the gel was stained with Coomassie Blue solution. After drying the stained gel on Whatman 3MM paper, ^{32}P incorporation was determined by film exposure.

Immunofluorescence microscopy

HeLa cells (or plasmids-transfected HeLa cells) were seeded on 8-well μ-Slides (#80826, Ibidi) at a density of 5×10^4 cells/well. The next day, the cells were washed with warm PBS and then fixed with 4% paraformaldehyde in PBS for 20 min at room temperature. After washing out with PBS, the cells were permeabilized with 0.1% Triton X-100 in PBS for 15 min at room temperature and then washed with PBS and blocked with Image-iT FX signal enhancer (#136933, Molecular Probes) for 30 min at room temperature. After blocking, the cells were washed with PBS and stained with the indicated primary antibodies at a ratio of 1:100 in 4% BSA/PBS for 2 h at room temperature followed by staining with secondary antibodies (goat anti-rabbit IgG–Alexa Fluor 488 (11008, Invitrogen), goat anti-rabbit IgG–Alexa Fluor 546 (A11010, Invitrogen), and goat anti-mouse IgG–Alexa Fluor 488 (A11001, Invitrogen)) at a ratio of 1:1000 in 4% BSA/PBS for 1 h at room temperature. After staining, the cells were washed with PBS and mounted in Fluoroshield mounting medium with DAPI (ab104139, Abcam). Fluorescence was detected using an LSM 880 laser-scanning microscope (Zeiss).

Proximity ligation assay

HeLa cells were seeded on 8-well μ-Slides at a densities of 5×10^4 cells/well. Cells were fixed, permeabilized, and stained with primary antibodies according to the method described above under "Immunofluorescence microscopy." A proximity ligation assay was performed using Duolink *in situ* red starter kit mouse/rabbit (DUO92101, Sigma-Aldrich) according to the manufacturer's instruction. The fluorescence signals were measured using a Zeiss LSM 880 laser-scanning microscope.

Statistical analysis

All data were obtained from at least three independent experiments and expressed as means ± S.D. Statistical analysis was performed using Microsoft Excel Student's *t* test (two-tailed), and $p < 0.05$ was considered significant.

Author contributions—J. H. C. conducted most of the experiments regarding the p90RSK–UBR5 pathway in the miRNA pathway, and S. A. K. worked mostly on the cloning and luciferase assays. Y. S. and S. G. P. supported the design of some of the experiments. B. C. P., J. K., and S. K. contributed to experimental design and supervision and, along with other authors, wrote the manuscript.

References

1. Carthew, R. W., and Sontheimer, E. J. (2009) Origins and mechanisms of miRNAs and siRNAs. *Cell* **136,** 642–655
2. Eulalio, A., Huntzinger, E., and Izaurralde, E. (2008) GW182 interaction with Argonaute is essential for miRNA-mediated translational repression and mRNA decay. *Nat. Struct. Mol. Biol.* **15,** 346–353
3. Braun, J. E., Huntzinger, E., Fauser, M., and Izaurralde, E. (2011) GW182 proteins directly recruit cytoplasmic deadenylase complexes to miRNA targets. *Mol. Cell* **44,** 120–133
4. Chu, C. Y., and Rana, T. M. (2006) Translation repression in human cells by microRNA-induced gene silencing requires RCK/p54. *PLoS Biol.* **4,** e210

5. Rouya, C., Siddiqui, N., Morita, M., Duchaine, T. F., Fabian, M. R., and Sonenberg, N. (2014) Human DDX6 effects miRNA-mediated gene silencing via direct binding to CNOT1. *RNA* **20,** 1398–1409
6. Zekri, L., Huntzinger, E., Heimstädt, S., and Izaurralde, E. (2009) The silencing domain of GW182 interacts with PABPC1 to promote translational repression and degradation of microRNA targets and is required for target release. *Mol. Cell. Biol.* **29,** 6220–6231
7. Sonenberg, N., and Hinnebusch, A. G. (2009) Regulation of translation initiation in eukaryotes: Mechanisms and biological targets. *Cell* **136,** 731–745
8. Callaghan, M. J., Russell, A. J., Woollatt, E., Sutherland, G. R., Sutherland, R. L., and Watts, C. K. (1998) Identification of a human HECT family protein with homology to the *Drosophila* tumor suppressor gene hyperplastic discs. *Oncogene* **17,** 3479–3491
9. Henderson, M. J., Russell, A. J., Hird, S., Muñoz, M., Clancy, J. L., Lehrbach, G. M., Calanni, S. T., Jans, D. A., Sutherland, R. L., and Watts, C. K. (2002) EDD, the human hyperplastic discs protein, has a role in progesterone receptor coactivation and potential involvement in DNA damage response. *J. Biol. Chem.* **277,** 26468–26478
10. Henderson, M. J., Munoz, M. A., Saunders, D. N., Clancy, J. L., Russell, A. J., Williams, B., Pappin, D., Khanna, K. K., Jackson, S. P., Sutherland, R. L., and Watts, C. K. (2006) EDD mediates DNA damage-induced activation of CHK2. *J. Biol. Chem.* **281,** 39990–40000
11. Honda, Y., Tojo, M., Matsuzaki, K., Anan, T., Matsumoto, M., Ando, M., Saya, H., and Nakao, M. (2002) Cooperation of HECT-domain ubiquitin ligase hHYD and DNA topoisomerase II-binding protein for DNA damage response. *J. Biol. Chem.* **277,** 3599–3605
12. Gudjonsson, T., Altmeyer, M., Savic, V., Toledo, L., Dinant, C., Grøfte, M., Bartkova, J., Poulsen, M., Oka, Y., Bekker-Jensen, S., Mailand, N., Neumann, B., Heriche, J. K., Shearer, R., Saunders, D., *et al.* (2012) TRIP12 and UBR5 suppress spreading of chromatin ubiquitylation at damaged chromosomes. *Cell* **150,** 697–709
13. Maddika, S., and Chen, J. (2009) Protein kinase DYRK2 is a scaffold that facilitates assembly of an E3 ligase. *Nat. Cell Biol.* **11,** 409–419
14. Jung, H. Y., Wang, X., Jun, S., and Park, J. I. (2013) Dyrk2-associated EDD-DDB1-VprBP E3 ligase inhibits telomerase by TERT degradation. *J. Biol. Chem.* **288,** 7252–7262
15. Benavides, M., Chow-Tsang, L. F., Zhang, J., and Zhong, H. (2013) The novel interaction between microspherule protein Msp58 and ubiquitin E3 ligase EDD regulates cell cycle progression. *Biochim. Biophys. Acta* **1833,** 21–32
16. Smits, V. A. (2012) EDD induces cell cycle arrest by increasing p53 levels. *Cell Cycle* **11,** 715–720
17. Chen, H. W., Yang, C. C., Hsieh, C. L., Liu, H., Lee, S. C., and Tan, B. C. (2013) A functional genomic approach reveals the transcriptional role of EDD in the expression and function of angiogenesis regulator ACVRL1. *Biochim. Biophys. Acta* **1829,** 1309–1319
18. Yoshida, M., Yoshida, K., Kozlov, G., Lim, N. S., De Crescenzo, G., Pang, Z., Berlanga, J. J., Kahvejian, A., Gehring, K., Wing, S. S., and Sonenberg, N. (2006) Poly(A) binding protein (PABP) homeostasis is mediated by the stability of its inhibitor, Paip2. *EMBO J.* **25,** 1934–1944
19. Rutz, S., Kayagaki, N., Phung, Q. T., Eidenschenk, C., Noubade, R., Wang, X., Lesch, J., Lu, R., Newton, K., Huang, O. W., Cochran, A. G., Vasser, M., Fauber, B. P., DeVoss, J., Webster, J., *et al.* (2015) Deubiquitinase DUBA is a post-translational brake on interleukin-17 production in T cells. *Nature* **518,** 417–421
20. Kayagaki, N., Phung, Q., Chan, S., Chaudhari, R., Quan, C., O'Rourke, K. M., Eby, M., Pietras, E., Cheng, G., Bazan, J. F., Zhang, Z., Arnott, D., and Dixit, V. M. (2007) DUBA: A deubiquitinase that regulates type I interferon production. *Science* **318,** 1628–1632
21. Kondo, T., Kawai, T., and Akira, S. (2012) Dissecting negative regulation of Toll-like receptor signaling. *Trends Immunol.* **33,** 449–458
22. Guo, B., and Cheng, G. (2007) Modulation of the interferon antiviral response by the TBK1/IKKi adaptor protein TANK. *J. Biol. Chem.* **282,** 11817–11826
23. Tseng, P. H., Matsuzawa, A., Zhang, W., Mino, T., Vignali, D. A., and Karin, M. (2010) Different modes of ubiquitination of the adaptor TRAF3 selectively activate the expression of type I interferons and proinflammatory cytokines. *Nat. Immunol.* **11,** 70–75
24. Perkins, D. J., Polumuri, S. K., Pennini, M. E., Lai, W., Xie, P., and Vogel, S. N. (2013) Reprogramming of murine macrophages through TLR2 confers viral resistance via TRAF3-mediated, enhanced interferon production. *PLoS Pathog.* **9,** e1003479
25. Mizushima, N. (2007) Autophagy: Process and function. *Genes Dev.* **21,** 2861–2873
26. Su, H., Meng, S., Lu, Y., Trombly, M. I., Chen, J., Lin, C., Turk, A., and Wang, X. (2011) Mammalian hyperplastic discs homolog EDD regulates miRNA-mediated gene silencing. *Mol. Cell* **43,** 97–109
27. Eulalio, A., Tritschler, F., and Izaurralde, E. (2009) The GW182 protein family in animal cells: New insights into domains required for miRNA-mediated gene silencing. *RNA* **15,** 1433–1442
28. Mishra, R., Chhatbar, C., and Singh, S. K. (2012) HIV-1 Tat C-mediated regulation of tumor necrosis factor receptor-associated factor-3 by microRNA 32 in human microglia. *J. Neuroinflammation* **9,** 131
29. Gu, H., Yu, J., Dong, D., Zhou, Q., Wang, J. Y., and Yang, P. (2015) The miR-322-TRAF3 circuit mediates the pro-apoptotic effect of high glucose on neural stem cells. *Toxicol. Sci.* **144,** 186–196
30. Hornbeck, P. V., Zhang, B., Murray, B., Kornhauser, J. M., Latham, V., and Skrzypek, E. (2015) PhosphoSitePlus, 2014: Mutations, PTMs and recalibrations. *Nucleic Acids Res.* **43,** D512–D520
31. Pearce, L. R., Komander, D., and Alessi, D. R. (2010) The nuts and bolts of AGC protein kinases. *Nat. Rev. Mol. Cell Biol.* **11,** 9–22
32. Frödin, M., Jensen, C. J., Merienne, K., and Gammeltoft, S. (2000) A phosphoserine-regulated docking site in the protein kinase RSK2 that recruits and activates PDK1. *EMBO J.* **19,** 2924–2934
33. Johnson, S. M., Grosshans, H., Shingara, J., Byrom, M., Jarvis, R., Cheng, A., Labourier, E., Reinert, K. L., Brown, D., and Slack, F. J. (2005) RAS is regulated by the let-7 microRNA family. *Cell* **120,** 635–647
34. Ding, L., and Han, M. (2007) GW182 family proteins are crucial for microRNA-mediated gene silencing. *Trends Cell Biol.* **17,** 411–416
35. Huang, O. W., Ma, X., Yin, J., Flinders, J., Maurer, T., Kayagaki, N., Phung, Q., Bosanac, I., Arnott, D., Dixit, V. M., Hymowitz, S. G., Starovasnik, M. A., and Cochran, A. G. (2012) Phosphorylation-dependent activity of the deubiquitinase DUBA. *Nat. Struct. Mol. Biol.* **19,** 171–175
36. Arthur, J. S., and Ley, S. C. (2013) Mitogen-activated protein kinases in innate immunity. *Nat. Rev. Immunol.* **13,** 679–692
37. Kaiser, F., Cook, D., Papoutsopoulou, S., Rajsbaum, R., Wu, X., Yang, H. T., Grant, S., Ricciardi-Castagnoli, P., Tsichlis, P. N., Ley, S. C., and O'Garra, A. (2009) TPL-2 negatively regulates interferon-β production in macrophages and myeloid dendritic cells. *J. Exp. Med.* **206,** 1863–1871
38. Anjum, R., and Blenis, J. (2008) The RSK family of kinases: Emerging roles in cellular signalling. *Nat. Rev. Mol. Cell Biol.* **9,** 747–758
39. Leung, A. K., and Sharp, P. A. (2010) MicroRNA functions in stress responses. *Mol. Cell* **40,** 205–215
40. Qi, H. H., Ongusaha, P. P., Myllyharju, J., Cheng, D., Pakkanen, O., Shi, Y., Lee, S. W., Peng, J., and Shi, Y. (2008) Prolyl 4-hydroxylation regulates Argonaute 2 stability. *Nature* **455,** 421–424
41. Zeng, Y., Sankala, H., Zhang, X., and Graves, P. R. (2008) Phosphorylation of Argonaute 2 at serine-387 facilitates its localization to processing bodies. *Biochem. J.* **413,** 429–436
42. Rüdel, S., Wang, Y., Lenobel, R., Körner, R., Hsiao, H. H., Urlaub, H., Patel, D., and Meister, G. (2011) Phosphorylation of human Argonaute proteins affects small RNA binding. *Nucleic Acids Res.* **39,** 2330–2343
43. Rybak, A., Fuchs, H., Hadian, K., Smirnova, L., Wulczyn, E. A., Michel, G., Nitsch, R., Krappmann, D., and Wulczyn, F. G. (2009) The let-7 target gene mouse lin-41 is a stem cell specific E3 ubiquitin ligase for the miRNA pathway protein Ago2. *Nat. Cell Biol.* **11,** 1411–1420

ASBMB